CHAPTER II
LITERATURE REVIEW

2.1 The role of the oxygen storage in the three-way catalysts (TWCs)

2.1.1 The role of the oxygen storage in the TWC efficiency

The advent, in the early 1980s, of the TWC has represented a major breakthrough in the development of the automotive pollution control devices As is well known, TWCs are capable of simultaneously and efficiently converting CO, hydrocarbon (HC) and NO_x into harmless CO_2, H_2O and N_2, provided that the air to-fuel ratio (A/F) is constantly kept in the exhaust at the stoichiometric point, i.e., under conditions where the amount of oxidants is equal to that of reducing agents. A/F is defined as

$$A/F = \frac{\text{mass of air consumed by the engine}}{\text{mass of fuel consumed by the engine}};$$

for stoichiometric combustion of isooctane (ideal fuel) A/F = 14.65 which represents the stoichiometric point. The engine-out exhaust gas composition is also commonly classified in terms of λ:

$$\lambda = \frac{\text{actual engine A/F}}{\text{stoichiometric engine A/F}}.$$

The fundamental relationship between the TWC efficiency and the oscillations in the air-to-fuel ratio is represented in Figure 2.1. A perusal of Figure 2.1 reveals some important aspects of the three-way catalysis that are; (i) due to the opposite nature of the reactions responsible for the removal of the pollutants, i.e. oxidation of HC and CO and simultaneous reduction of NO_x, the conversions required by the legislation (< 95%) are attained only in a narrow window of A/F, close to the stoichiometric point; (ii) strong deviations/oscillations of A/F from the stoichiometric point lead to widening of the operating A/F window resulting in an average poor performance of the TWCs.

It is worth recalling that uncontrolled emissions of 40-60 g of CO/km were common to most of the passenger vehicles by the end of the 60s; this amount decreased to 2.3 g CO/km in 2000 and will be phased down to 1 g of CO/km in 2005 by European legislation (Euro phases 3 and 4). These limits therefore represent reduction of respectively 94-96% and 97-98% compared to uncontrolled emissions. US Tier 2 legislation, issued by EPA, challenged even more the catalyst/vehicle producers: besides the quite restrictive limits on the emissions, durability as high as 120,000 miles (about 200,000 km) will be phased-in by 2004. Clearly, an extreme efficiency and durability is nowadays required to the TWCs (Shelef and McCabe, 2000). As illustrated in Figure 2.1, such high efficiency is achieved over TWCs in a very narrow A/F window, which requires a highly efficient control of the exhaust composition, in particular in terms of residual oxygen concentration.

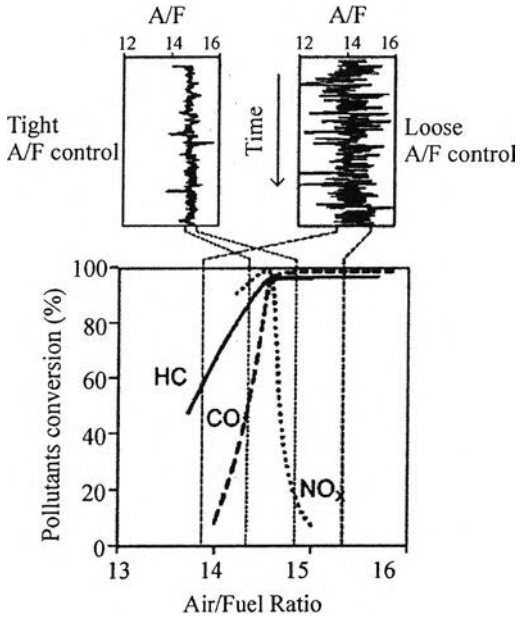

Figure 2.1 Relationship between the oscillations in the A/F in the exhaust and TWC efficiency.

An integrated strategy is employed to control A/F under operating conditions (Figure 2.2), which is based on (i) an ''engineering control'' of the A/F using an integrated electronic system that controls fuel and air injection using a feedback signal by continuously monitoring the oxygen concentration in the exhaust with a λ (oxygen) sensor, (ii) a ''chemical control'' of A/F, which is achieved by adding a CeO_2-containing promoter of the so-called OSC. The latter component is added because of its ability to absorb and release oxygen under, respectively, fuel-lean and fuel-rich conditions, according to the reaction:

$$CeO_2 \underset{H_2O/CO_2}{\overset{H_2/CO}{\rightleftharpoons}} CeO_{2-x} + x/2O_2 \qquad (1)$$

The definition of the OSC, i.e. capability to store and release oxygen, ignores a fundamental aspect of the OSC that is the nature of the oxidizing and reducing agents that may interact with the CeO_2 moiety.

Equation (1) therefore presents a very simplified picture of the redox behavior of the CeO_2-containing promoters under the exhaust conditions, due to the presence of continuously changing reaction conditions and presence of a variety of oxidants/reductants, e.g., H_2O, CO_2, CO, HC, H_2, that easily interfere with the pure redox process (Otsuka *et al.*, 1983).

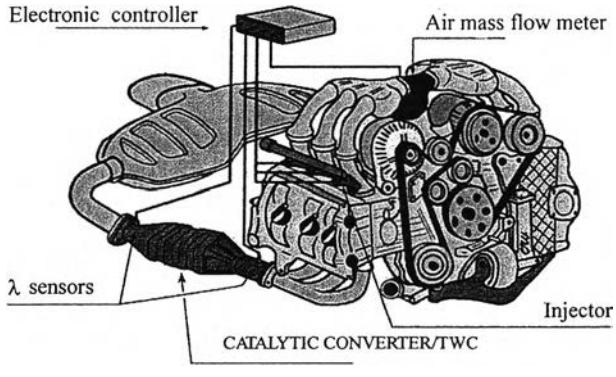

Figure 2.2 Modern TWC/engine/oxygen sensor (λ) control loop for engine exhaust control.

An important corollary of these observations is that the extent of A/F oscillations plays a fundamental role in the efficiency and hence detection of efficiency of the TWCs. As shown in Figure 2.2, monitoring of A/F is continuously performed by the λ sensors at the inlet and outlet of the catalytic converter. In the absence of the OSC function, comparable fluctuation of A/F is expected at both λ sensors, whereas the presence of an efficient OSC promoter results in a dampening of the fluctuation at the outlet, as a result of the buffering capacity (Equation (1)). Wide fluctuation in the O_2 concentration detected by the second λ sensor signal is indicative of deactivation of the OSC promoter and is correlated to the catalyst efficiency.

Figure 2.3 shows an example of a correlation between the OSC and the TWC efficiency (Taha *et al.*, 1998). Even though a simple correlation is not found, the precise nature of these correlations is in fact related to the particular engine-engine control-TWC system used, and monitoring OSC efficiency using the λ sensor is employed as a measure of the TWC performance. This is indeed the principle, which most of the current on-board diagnostics (OBD) technologies employ to detect deactivation/failure of the TWCs (Sideris, 1997).

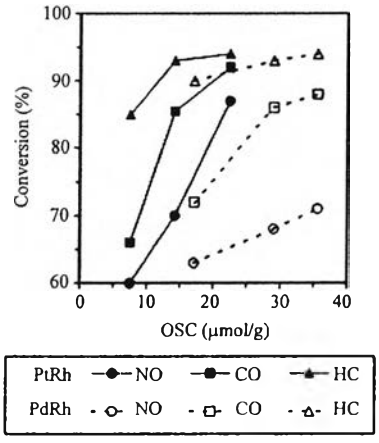

Figure 2.3 Correlation between the catalytic efficiency of PtRh and PdRh catalysts engine-bench aged for 25, 50 and 200 h (T_{max} 950°C) and the OSC measured by alternating CO/O_2 pulses: conversion of the different pollutants (NO, CO and HC) are given over PtRh and PdRh as a function of CO-OSC.

In summary, the efficiency of the TWCs is unambiguously related to the efficiency of the OSC function: loss of OSC signals deactivation of the TWC.

2.1.2 Measurement of OSC

According to Equation (1), the oxygen storage is formally considered as the amount of oxygen released (left-to-right) or stored (right-to-left) under the rich (net reducing)/lean (net oxidizing) excursions of A/F.

From the thermodynamic point of view, the standard potential for reduction of Ce^{4+} to Ce^{3+} is 1.74 V in solution (Moeller, 1982) which indicates that Ce(IV) in solution is a strong oxidant. In the solid state, the situation is different. CeO_2 crystallizes in the fluorite structure in which each cerium ion is co-ordinate by eight oxygen neighbors. This co-ordination stabilizes the Ce^{4+} state and makes the reduction of CeO_2 unfavorable. In fact, the fluorite structure of ceria is a direct result of the ionic nature of ceria and of the charge and size of the ions. Model calculation has shown that it is formed when a sufficiently high number of CeO_2 units (about 50) are clustered together (Cordatos, 1996). The ability of CeO_2 to undergo a relatively easy reduction (*vide infra*) compared to other oxides, can in principle also be related to the general property of fluorite structure/mixed valence oxides to strongly deviate from stoichiometry (Killner and Steele, 1981). It is worth recalling that of the two processes (reduction/oxidation), oxidation is fast (Holmgren and Andersson, 1998), and occurs deep into the bulk even at room temperature (RT), whereas reduction typically occurs above 473 K (Perrichon *et al.*, 1994).

Two types of measurements of OSC were distinguished by Yao and Yu Yao (1984): the so-called complete or ultimate oxygen storage capacity (total OSC), i.e. an oxygen storage measured under thermodynamic control (*vide infra*); and the kinetic oxygen storage, (dynamic OSC), i.e. measured under kinetic control.

The total OSC represents the widest ''limiting'' amount of oxygen transferable from the catalyst at a given temperature and generally is limited in the case of CeO_2 by formation of some non-stoichiometric CeO_{2-x} compound (Perrichon *et al.*, 1994 and Ricken *et al.*, 1984). Consistently, isothermal reduction of CeO_2 at 973 and 773 K led respectively to $CeO_{1.8}$ and $CeO_{1.89}$ (Fierro *et al.*, 1987). Total OSC is typically measured using the temperature programmed reduction (TPR)

technique or by an oxidation following a reduction at a fixed temperature (Boaro *et al.*, 2003).

The dynamic OSC is typically measured by alternatively injecting pulses of an oxidizing, usually O_2 in inert gas, and reducing, usually CO or H_2 in inert gas or even inert gas itself at a high temperature (Bernal *et al.*, 1997), mixtures into a flow of inert carrier passing through the catalysts bed at a fixed temperature. It is considered to be more related to the real exhaust conditions, since O_2 release/accumulation is measured under dynamic conditions; on the other hand, standard conditions for these measurements are lacking so that comparing data from different sources is difficult. Also the fact that the redox cycles are often much slower compared to the rate of A/F (1 Hz) oscillations due to physical constraints, are factors that make this technique much less used compared to the traditional and readily available TPR technique.

It is important to underline the point that correlations between the dynamic OSC and total OSC have been found. Also worth to be noticed that, as shown below, the nature of the reducing agent plays a key role in the OSC. Accordingly, in the following text the H_2- and CO-OSC will be distinguished to indicate whether hydrogen or carbon monoxide has been used as reducing agent. In fact, HC have only sparingly been employed as reducing agent, more complex reaction does in fact occur on the surface in this case, rather than a pure redox process (Kaspar *et al.*, 2000).

2.1.3 Role and mechanism of the OSC

As shown in Section 2.1.1, the OSC is a crucial property of the TWCs directly linked to its efficiency. However, it is important to recognize that the impact of OSC on the catalytic performance of the TWC cannot be limited to a pure oxygen buffering effect as indicated by the redox process reported in Equation (1). In fact, it is an ambitious task to define the role of the CeO_2 in the three-way catalysis since evidence for multiple effects of this promoter have been found. Ceria has been suggested to:

- promote the noble metal dispersion;
- increase the thermal stability of the Al_2O_3 support;

- promote the water gas shift (WGS) and steam reforming reactions;
- favor catalytic activity at the interfacial metal-support sites;
- promote CO removal through oxidation employing lattice oxygen;
- Store and release oxygen under respectively lean and rich conditions.

A perusal of the above listed effects suggests, however, that there is a common point in most of the chemical effects, which are related to the role of NM/CeO_2 (NM = noble metal) system in the TWCs. This is to promote under the reaction conditions, the rate of migration/exchange of oxygen species between the different reactants. Under such a broad perspective, most of the above quoted promoting phenomena can be somehow related to Equation (1). The promotion of the WGS by CeO_2 can be cited in this respect as an example (Bunluesin *et al.*, 1998). Two reaction pathways were proposed for this reaction (Shido and Iwasawa, 1993): an ''associative'' mechanism in which a hydroxyl group produced by dissociation of water can combine with an adsorbed carbon monoxide to further react to give CO_2 and H_2 via a formate intermediate and a ''regenerative'' mechanism, where water oxidizes the surface producing hydrogen and an oxidized surface capable of interacting with CO to give CO_2. The discrepancy between the two proposals can be accounted for when a bi-functional mechanism is considered for the NM/CeO_2 systems where, in addition to the reaction catalyzed at the NM sites, a reaction path is considered that involves a reaction between CO adsorbed on the NM and oxygen from CeO_2 at the NM/CeO_2 interface (Bunluesin *et al.*, 1998).

The reaction mechanism is generally investigated under stationary feed stream where the occurrence of a ''regenerative'', i.e. redox type of reaction mechanism is less likely, whereas occurrence of such a mechanism is highly probable under a feed stream cycled between oxidizing and reducing conditions, where reduction/oxidation of CeO_2 sites can effectively occur. Consistently, TWC activity of a model $Pt/CeO_2/Al_2O_3$ catalyst was much more effectively promoted when water was added to the simulated exhaust mixture under cycled feed stream compared to stationary streams, either reducing or oxidizing (González-Velasco *et al.*, 1997). Under cycled conditions, most of the reduced ceria moiety is oxidized by

water in the exhaust, generating H_2 (González-Velasco *et al.*, 1997). Production of H_2 under reaction condition is an important aspect as NO_x reduction is very fast when H_2 is used as reducing agent even under oxidizing conditions (lean $DeNO_x$) (Burch and Coleman, 1999) and, in addition, it promotes removal of adsorbed SO_x (Hirata *et al.*, 2001).

These considerations indicate that OSC may be considered as a complex phenomenon in that the pure redox process (Equation (1)) can hardly be considered apart from the whole reaction network that occurs under the exhaust conditions, as many of the chemical reactions are intimately linked together. On the other hand, it has been unequivocally shown that catalytic properties, in particular those of CeO_2 and NM/CeO_2, are directly linked to the reducibility of CeO_2 at low temperature (□ 770 K) (Kapar *et al.*, 1999).

As shown in Figure 2.4, upon redox aging at 1000°C, both CeO_2 and Rh/CeO_2 strongly sinter with surface area dropping below 10 m^2 g^{-1}. Fresh samples feature the typical two reduction peak TPR profile where the low temperature (LT, < 800 K) peak is associated with reduction of the surface whereas the peak at high temperature (HT, ≈1100 K) is associated with reduction in the bulk of CeO_2 (Johnson and Mooi, 1987). In the presence of the NM, the LT peak shifts down to 450 K, which is associated with the ability of Rh to activate and spill hydrogen over the support thus facilitating surface reduction.

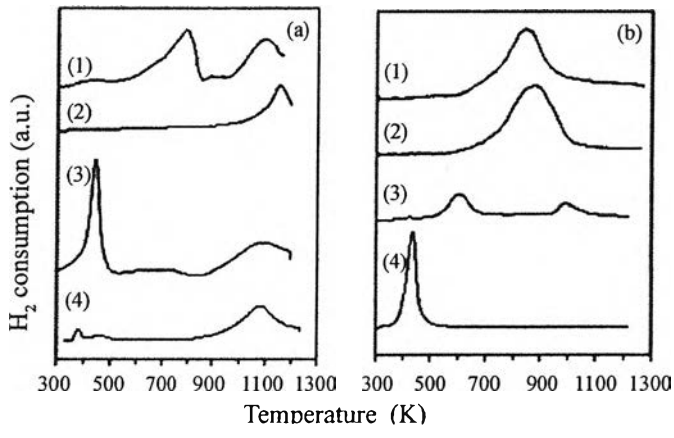

Figure 2.4 Effect of redox ageing on the H_2-TPR profiles of (a) CeO_2 (Kapar and Fornasiero, 2003) and Rh/CeO_2 (Heck and Farrauto, 1995). Surface areas: fresh: 190

$m^2 g^{-1}$ (Kapar and Fornasiero, 2003) and redox-aged: <10 $m^2 g^{-1}$ (Heck and Farrauto, 1995); (b) $Ce_{0.5}Zr_{0.5}O_2$ (Kapar and Fornasiero, 2003) and Rh/ $Ce_{0.5}Zr_{0.5}O_2$ (Farrauto *et al.*, 1995); Surface areas: fresh: 65 $m^2 g^{-1}$ (Kapar and Fornasiero, 2003), redox-aged: <10 $m^2 g^{-1}$ (Heck and Farrauto, 1995) and calcined 1873 K <10 $m^2 g^{-1}$) (Farrauto *et al.*, 1995) (adapted from (Kapar *et al.*, 2000)). The peak at 1000 K in fresh $Rh/Ce_{0.5}Zr_{0.5}O_2$ is attributed to reduction of some CeO_2 not incorporated into the solid solution.

In reality, more complex processes occur during the TPR experiment. Due to poor thermal stability of CeO_2 under a reducing atmosphere (Perrichon *et al.*, 1995), sintering of the high surface area material occurs concurrently to the reduction process. As a consequence of the loss of surface area (sintering), the low temperature reduction peaks disappear in the TPR profile of the aged sample.

Notice that also the NM-CeO_2 interaction, detected by the shift of the LT peak to lower temperature, is no longer detected in the aged samples indicating permanent loss of LT reduction capability, i.e. total OSC. The critical importance of the extent of the surface area of CeO_2 for the low temperature redox processes suggested that at the usual converter working temperatures, and under the periodic A/F operations, redox processes in a NM/CeO_2 system are essentially limited to the surface. These observations immediately point out the major issue of the late 1980s and early 1990s TWCs, which was the thermal stability of the surface area of the CeO_2 promoter: a drop in the CeO_2 surface area is directly related to catalyst deactivation.

2.2 Thermal stability and redox properties of CeO_2-ZrO_2 mixed oxides

The increasing restrictions for the standards for the automotive emissions have set new challenges for the development of the new automotive TWCs. In fact, a major problem of the TWC converters is that significant conversions are attained only at high temperatures (>600 K). As a result, during the cold-start of the engine, the emissions of the pollutants, particularly the HC, are quite high until the converter reaches the operating temperature. Accordingly, inclusion of the cold-start in the

engine test and the remarkably low limits required in the near future for the HC emissions demanded for the development of the so-called close coupled catalyst (CCC). These catalysts, being manifold mounted, experience temperatures up to 1273±1373 K, which requires an extremely high thermal resistance.

As described above, thermal stabilities up to 1373K are required for future TWC applications. CeO_2-ZrO_2 mixed oxides are employed as the OSC component in modern TWCs, due to their excellent redox behavior and higher thermal stability compared to the traditionally employed CeO_2 (Fornasiero *et al.*, 1996). Nowadays, there is a general agreement that the presence of a single-phase solid solution is preferable compared to microdomain-or phase-segregated non-homogeneous CeO_2-ZrO_2 mixed oxides, as the former systems generally lead to better textural stability and redox properties (Kapar *et al.*, 1999), even though some contradictory indications exist (Egami *et al.*, 1997). In addition to high activity and cost-effectiveness, durability is the most important property of a TWC; accordingly it is expected that a single-phase product should feature less modification during its lifetime in the converter. As shown in Equation (2), ZrO_2 exists as a monoclinic phase at ambient pressure and below 1400 K. Tetragonal and cubic phases are formed at very high temperatures (Yasima *et al.*, 1996):

$$\underset{P2_1/c}{\text{Monoclinic}} \overset{1400\,\text{K}}{\leftrightarrow} \underset{P4_2/mmc}{\text{Tetragonal}} \overset{2640\,\text{K}}{\leftrightarrow} \underset{Fm\bar{3}m}{\text{Cubic}} \qquad (2)$$

In contrast, CeO_2 crystallizes in the fluorite structure (space group Fm3m). Given the relatively large difference (13%) between the cation radii of Ce^{4+} (0.097 nm) and Zr^{4+} (0.084 nm), a limited mutual solubility might be expected (West, 1999). Consistently, only the t- and c-phase, found, respectively, at high (>80 mol %) and low (<20 mol %) ZrO_2 contents are thermodynamically stable, while two meta-stable tetragonal phases (t', t'') were detected at intermediate compositions (Figure 2.5) (Yashima *et al.*, 1994). The exact location of the meta-stable boundary between the t' and t'' is still undefined and appears to depend on different parameters, particle size included (Kapa *et al.*, 1999 and Fornasiero *et al.*, 1996).

The presence of meta-stable phases poses serious difficulties to researchers - sometimes underestimated - when the homogeneity of the prepared mixed oxide has to be assessed. Vegards rule is typically applied to assess the presence of solid solution. Due to lower Zr^{4+} cation radius compared to Ce^{4+}; linear decreases of the cell parameter (or cell volume, when t-phases are included) is expected and, in fact, observed (Otsuka *et al.*, 1999).

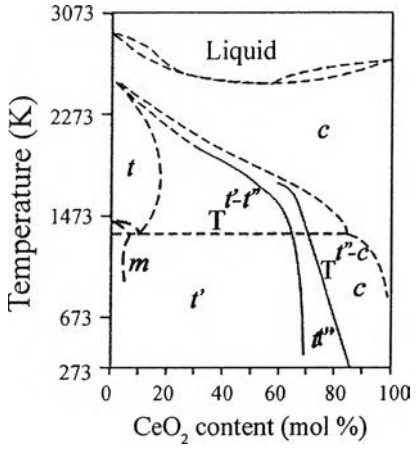

Figure 2.5 CeO_2-ZrO_2 phase diagram: the metastable (t', t'') phase boundaries are included.

The as-synthesized high-surface area samples typically feature quite broad X-ray diffraction (XRD) peaks, due to the nanometric dimension of the crystallites. The observed phase segregation may often be related to the presence of compositional inhomogeneities generated by the synthesis method, rather than induced by calcination.

2.3 Synthesis methodologies

An adequate synthesis methodology is a fundamental starting point for developing any new material. As emphasized above, for TWCs application the synthesis must confer to the CeO_2-ZrO_2-based materials the following properties:

- High thermal stability of the textural properties;

- Formation of a single-phase product;
- Suitable redox properties, the reduction at low temperatures being considered as a desirable property.

A cost-effective solution should be always considered for large-scale applications. A great variety of methods have been investigated aiming at improving the above-quoted properties as shown below:

- solid-state synthesis (Eguchi *et al.*, 2000)
- high-energy milling (Leitenburg *et al.*, 1995)
- coprecipitation
- room-temperature coprecipitation (Hori *et al.*, 1999)
- medium-to-high temperatures coprecipitation (Oliveira and Torem, 2001)
- surfactant-modified coprecipitation (Terribile *et al.*, 1998)
- ultrasound-induced coprecipitation (Yin *et al.*, 2002)
- microemulsion precipitation (Oliveira and Torem, 2001)
- spray hydrolysis (Djurado and Meunier, 1998)
- combustion synthesis (Aruna and Patil, 1998)
- electrochemical coprecipitation (Mukherjee *et al.*, 2001)
- chemical vapor deposition (Barreca *et al.*, 2001)
- sol–gel (like) synthesis
- alkoxide precursors (Fornasiero *et al.*, 1996 and Rossignol *et al.*, 1999)
- oxalic acid (Settu and Gobinathan, 1996)
- citric acid (Vidmar *et al.*, 1997)
- polyacrylic acid (Oliveira and Torem, 2001)
- hydrazine (Hirono *et al.*, 1995)
- poly-alcohols (Yamamoto *et al.*, 2000)
- urea (Thammachrt *et al.*, 2001)

As far as the solid-state synthesis and high-energy milling are concerned, these types of synthesis lead to preparation of ceramics, which, by the way, is a field where stabilized zirconias are largely employed. Ceramic materials feature a high degree of densification and therefore sintering, which is exactly the opposite of what

is the desirable property for catalytic applications; hence, these syntheses will not be further considered.

Due to the lack of a generally recognized criterion for detection of the homogeneity of the mixed oxide, a comparison of the different synthesis routes is not easy. The sol-gel syntheses by controlled hydrolysis of alkoxide or similar precursors are considered to be a suitable method leading to high degree of homogeneity when mixed oxides are prepared. The underlying idea is that the preparation of the gel or gel-like precursor should lead to a homogeneous dispersion at molecular level of the Ce and Zr species, which then upon calcination lead to an intimately mixed oxide. However, it should be taken into account that when the rates of hydrolysis between the two metals are quite different, such as in the case of CeO_2 and ZrO_2 precursors, it may be quite difficult to simultaneously hydrolyze both precursors, particularly when $Zr(n\text{-}PrOH)_4$ is employed as a precursor. $Zr(n\text{-}PrOH)_4$ in fact rapidly reacts, even with air humidity, unless appropriate chemical modifications of the hydrolyzing process are adopted such as addition of acetylacetone which controls the rate of hydrolysis (Chatry *et al.*, 1994). Even the choice of the solvent where the hydrolysis is performed, e.g. alcohols with different chain lengths, was shown to affect the nature of the product in the case of ZrO_2 (Caracoche *et al.*, 2000). In line with this consideration, application of the sol-gel methodology often led to detection of in-homogeneities, phase segregation, or presence of different phases even after relatively mild calcination as detected by the asymmetry of the diffraction peaks (Fornasiero *et al.*, 1996). It should be noted, however, that when the experimental conditions of this process are optimized, the homogeneity of the mixed oxide can be improved (Rossignol *et al.*, 1999).

A large number of preparations were performed by using organic complexion agents to generate a gel-like type of resins where homogeneous dispersion of the metal cations can, in principle, be achieved. Typically citric or oxalic acid, in the presence/absence of polyvinyl alcohol, are employed as complexion agents (Settu and Gobinathan, 1996). Rapid heating of the products obtained by this method leads to solids with appreciable surface area. This makes segregations in the oxide precursor unfavorable, which makes this synthesis method attractive for preparation of solid solutions. However, the choice of the experimental

conditions is critical as the formation of the gel was affected even by the relative atmospheric humidity which apparently modified the rates of formation of the sol and the gel (Settu and Gobinathan, 1996).

The combustion synthesis (Aruna and Patil, 1998) can be related to the citrate route in that also in this case an extremely rapid thermal decomposition of the ''fuel-containing'' solution of precursors is the key step conferring a homogeneous nature to the resulting product. Due to the high temperature experienced by the solid in the combustion, thermally stable products are in principle obtained. Thus, even complex oxides could be prepared by flame pyrolysis producing thermally stable materials with appreciable surface area (Leanza *et al.*, 2000).

The direct room-temperature precipitation methods also presents challenges as it appears difficult to find appropriate co-precipitation conditions for different CeO_2-ZrO_2 compositions even in the case of commercial products (Cuif *et al.*, 1997). Thus, Hori *et al.* claimed that formation of homogenous solid solution can be attained by co-precipitation of Zr and Ce nitrates, however, when these samples were calcined at 1273 K for 2 h, significant phase segregation occurred (Hori *et al.*, 1998). This was confirmed in a subsequent study where the presence of two phases was invariably detected when a co-precipitation method was employed (Rossignol *et al.*, 1999). Reverse precipitation method has also been employed for the preparation of CeO_2-ZrO_2 mixed oxides (Bozo *et al.*, 2000), apparently giving better phase homogeneity compared to the direct precipitation, even though some phase segregation was detected after calcination at 1273 K (Bozo *et al.*, 2000).

The recognition that fast quenching/precipitation may represent a key factor in producing homogeneous solid led to application of high-temperature hydrothermal synthesis methods. This methodology has long been applied to ZrO_2-containing co-precipitated products to increase the sample homogeneity and textural stability, also allowing tuning the crystal morphology/size, an important property for the preparation of high-performance ceramic materials (Tani *et al.*, 1983). Chuah *et al.* have investigated in detail the effects of conditions of hydrothermal treatment on the precipitated cakes, showing an important influence of these factors on the textural properties (Chuah *et al.*, 1998). The rate of hydrolysis increases with temperature (Rabenau, 1985), which allows to ''force'' the hydrolysis and precipitation of the

oxide even at relatively low temperature and acidic conditions (Hirano *et al.*, 2001). Hirano and coworkers have investigated this kind of synthesis in detail showing that ultrafine CeO_2-containing particles may be effectively prepared (Hirano and Kato, 1999) and these products can feature quite remarkably high surface area even after heat treatment at 1273 K (Hirano *et al.*, 2001). At very high-near water critical-temperatures, the rate of hydrolysis becomes extremely rapid, which allowed to develop a continuous flow-through reactor to efficiently produce mixed oxides with various compositions and different particle morphology, according to the reaction temperature and feeding conditions (Darab and Matson, 1998). Recently, this technique has been extended to the preparation of CeO_2-ZrO_2 mixed oxides as well (Cabanas *et al.*, 2001).

In summary, there are a number of issues concerning the preparation of these apparently simple oxides, however, by appropriately designing the synthesis conditions and methodology; homogeneous nano-dispersed CeO_2-ZrO_2 solid solutions have been successfully obtained.

For TWC application, however, besides the homogeneity of the mixed oxide, textural stability is fairly important. Even though early studies showed that due to the strong modification of the oxygen sub lattice (Vlaic *et al.*, 1997), redox processes can occur in the bulk of these oxides at low temperatures even when sintered at 1873 K (Fornasiero *et al.*, 1995), the stability of the surface area is an important issue. A comparison of CO and H_2 as reducing agents under dynamic conditions clearly revealed that for the latter, the OSC occurs at the surface via a spillover mechanism at room temperature in the presence of reduced noble metal, whilst the reduction occurs deep into the bulk at temperatures as low as 373-473 K (Hickey *et al.*, 2000).

In contrast, when CO is employed as the reducing agent, the redox processes occur at higher temperatures, but, more importantly, the extent of CO-OSC is related to the surface area of the CeO_2-ZrO_2 mixed oxide, surface reactions being the rate-limiting processes in this case (Hickey *et al.*, 2000). A non-exhaustive survey of surface BET areas obtained for different CeO_2-ZrO_2 mixed oxides prepared by different synthesis routes is reported in Table 2.1. Care should be taken when such comparison is made due to the different synthesis conditions employed among

the various researchers, however, the effect of insertion of ZrO_2 into the CeO_2 lattice is clearly confirmed also by these recent data gathered from the literature, high ZrO_2 content favoring highest textural stability under equivalent synthesis conditions. This can be related to a retarding effect of ZrO_2 insertion into the CeO_2 lattice on the rate of sintering of the oxide (Janvier *et al.*, 1998).

Another observation is that the use of a sol-gel route resulted in a better textural stability compared to the co-precipitation technique for a $Ce_{0.9}Zr_{0.1}O_2$ (Table 2.1), which can be related to a better phase homogeneity achieved by the former synthesis method (Sun and Sermon, 1996). This result again stresses the necessity of designing an appropriate synthesis strategy to achieve a homogeneous solid solution as a product.

With the aim of addressing the issue of surface area, preparation of mesoporous solids by addition of surfactants in the synthesis has been attempted by some authors (Kapoor *et al.*, 2001). At variance with ZrO_2-based materials where assessed synthesis methodologies to produce meso-porous materials have been developed (Ying *et al.*, 1999), these attempts to produce such ordered CeO_2-ZrO_2 meso-porous systems were partly successful (Kapoor *et al.*, 2001).

Table 2.1 Effect of calcination temperature and time on BET surface areas of CeO_2 and CeO_2-ZrO_2 mixed oxides

Composition	Synthesis method	Calcination conditions and BET surface area				Refs./notes
		Temp./time	BET area	Temp./time	BET area	
CeO_2	Co-precpt.	823K/2h	55	973K/2h	5	de Leitenburg *et al.* 1996
$Ce_{0.8}Zr_{0.2}O_2$	Co-precpt.	823K/2h	85	973K/2h	30	de Leitenburg *et al.* 1996
$Ce_{0.83}Zr_{0.17}O_2$	Co-precpt.	773K/6h	85	973K/6h	58	Bozo *et al.* 2000, $3m^2g^{-1}$ (1273K, 6h)
$Ce_{0.67}Zr_{0.33}O_2$	Co-precpt.	773K/6h	104	973K/6h	70	Bozo *et al.* 2000, $8m^2g^{-1}$ (1273K, 6h)
$Ce_{0.90}Zr_{0.10}O_2$	Co-precpt.	1053K/4h	25	1173K/4h	18	Rossignol *et al.* 1999
	Sol-gel	1053K/4h	56	1173K/4h	35	Rossignol *et al.* 1999
$Ce_{0.75}Zr_{0.25}O_2$	Co-precpt.	773K/1h	72	1273K/4h	14	Hori *et al.* 1998
$Ce_{0.83}Zr_{0.17}O_2$	Co-precpt.	773K/1h	87	1273K/4h	14	Hori *et al.* 1998
$Ce_{0.5}Zr_{0.5}O_2$	Co-precpt. At 573 K	573K	105	1273K/1h	15	Cabanas et al. 2001
$Ce_{0.2}Zr_{0.8}O_2$	Co-precpt. At 373 K			1273K/	50	Hirano *et al.* 2001
$Ce_{0.6}Zr_{0.4}O_2$	Co-precpt. At 373 K			1273K/	43	Hirano *et al.* 2001
$Ce_{0.8}Zr_{0.2}O_2$	Co-precpt. At 373 K			1273K/	33	Hirano *et al.* 2001
$Ce_{0.8}Zr_{0.2}O_2$	Co-precpt./organic template	723K/2h	209	173K/2h	56	Terribile *et al.* 1998
$Ce_{0.5}Zr_{0.5}O_2$	Cellulose template	1073K/2h	129	1323K/12h	30	Shigapov *et al.* 2001

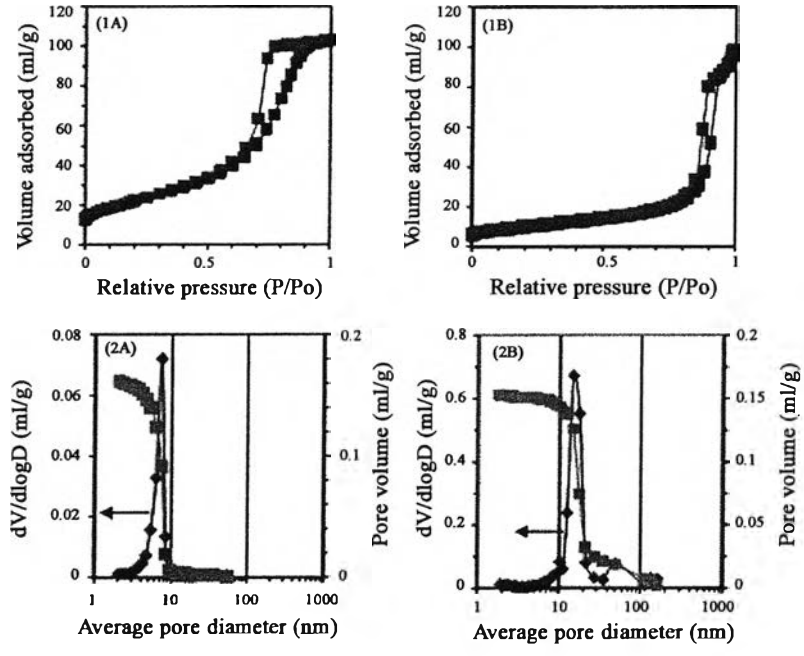

Figure 2.6 N_2 adsorption isotherm (1) and cumulative pore volume and pore distribution (2) as detected from N_2 desorption isotherm using the BJH method on two samples (A and B) single-phase $Ce_{0.8}Zr_{0.2}O_2$ solid solution (Kaspar *et al.*, 2001) (courtesy of MEL Chemical, Manchester, UK).

Materials with high surface area (200-300 m^2 g^{-1}) could, in fact, be prepared, however, when the calcinations temperature was increased above 1073 K, strong, decline of BET surface area was observed (Terribile *et al.*, 1998). In fact, despite the high surface area of these products, comparable sintering rates were observed in samples either conventionally co-precipitated or co-precipitated by a template-assisted route (Kaspar *et al.*, 1999).

An interesting exception is the use of cellulose as templating aent, recently reported by researchers from Ford Motor Co. (Shigapov *et al.*, 2001) that showed that by adsorbing the precursors on the surface of different kind of papers, the morphology of the obtained product closely follows that of the starting cellulose-containing material. Thus, filamentous particles of CeO_2-ZrO_2 mixed oxides were observed by SEM that closely resembled the morphology of the starting cellulose. Such morphology of the particles adversely affected the sintering process, allowing BET surface areas as high as 30 m^2 g^{-1} after calcination at 1323 K to be obtained.

These data clearly reveal that the design of the pore structure also plays a key role in enhancing the thermal stability of the CeO_2-ZrO_2 materials. The importance of, this aspect is clearly exemplified in Figure 2.6, where the pore distribution is shown for two samples of single-phase $Ce_{0.8}Zr_{0.2}O_2$ products, as checked by Rietveld analysis after calcination at 1273 K. Both samples were prepared to feature comparable BET areas (sample A: 27 m^2 g^{-1} and B: 35 m^2 g^{-1}), however, sample B was purposely synthesized in such a way to feature a pore distribution centered at pore radii significantly higher compared to sample A. When these samples were calcined at 1273K for 5 h, the surface area of sample A collapsed to 4 m^2 g^{-1}, whilst an appreciable value of 22 m^2 g^{-1} was measured over sample B.

This accounts for a relative decrease of surface area of 85% and 37%, respectively, for samples A and B. In terms of durability of the TWCs, clearly the behavior observed for sample B is more desirable because such relatively small drop of surface area after calcination at 1273 K suggests that negligible loss of precious metal due to metal particle encapsulation should occur in this case. Metal particle encapsulation upon aging at high temperatures was indeed shown to be an important pathway leading to deactivation of the model CeO_2-ZrO_2 containing TWCs (Graham *et al.*, 1999).

The investigation of the reduction behavior and dynamic-OSC, using both CO and H_2 as reducing agents disclosed remarkably different behaviors between the two samples, as exemplified in Figure 2.7 where the effects of severe and mild oxidation pre-treatments of the TPR profile are reported.

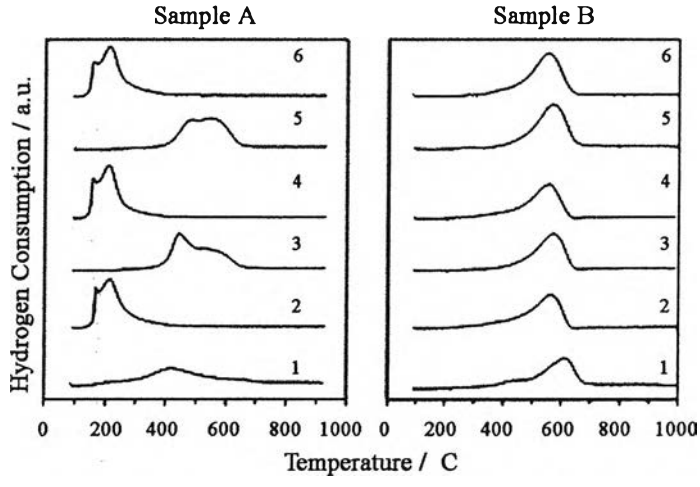

Figure 2.7 Temperature-programmed reduction profiles of single-phase $Ce_{0.8}Zr_{0.2}O_2$ samples with different textural properties (samples A and B from Figure 2.6, calcined at 1273 K for 5 h): effects of pre-treatments/redox aging. A severe oxidation at 1173 K (SO) precedes third and fifth TPR profiles, while mild oxidation at 700K precedes all the other TPR runs.

Previous works have shown that reduction behavior of CeO_2-ZrO_2 is strongly affected by the temperature of the pre-oxidation performed before the TPR run: a mild oxidation generates a low-temperature reduction profile whereas the severe-high-temperature oxidation generates a high-temperature reduction profile, both the reduction phenomena being reversibly inter-converted (Baker *et al.*, 1999). The reduction behavior of sample A, shown in Figure 2.7, illustrates this kind of modifiable reduction behavior. The exact origin of this sensitivity to the pre-treatment is still unclear even if the sintering of the mixed oxides leading to surface cerium enrichment was recently indicated as a pre-requisite to obtain this kind of variable reduction behavior (Fornasiero *et al.*, 2002). In agreement with this

observation, the texturally stable sample B features an almost constant-pre-treatment independent-reduction behavior (Figure 2.7). More importantly, sample B showed significantly better performances under the dynamic OSC conditions, i.e., conditions that are closer to the real exhaust conditions than a TPR run, compared to sample A (Kaspar *et al.*, 2001). This confirms an important role of the textural stability on the redox properties, in addition to those structural (Fornasiero *et al.*, 1995).

2.4 Sol-gel technology

A process that has, in the past years, gained much notoriety in the glass and ceramic fields is the sol-gel reaction. This chemistry produces a variety of inorganic networks from silicon or metal alkoxide monomer precursors. Although first discovered in the late 1800s and extensively studied since the early 1930s, a renewed interest (Hench and West, 1990) surfaced in the early 1970s when monolithic inorganic gels were formed at low temperatures and converted to glasses without a high temperature melting process (Brinker and Scherer, 1990).

Through this process, homogeneous inorganic oxide materials with desirable properties of hardness, optical transparency, chemical durability, tailored porosity, and thermal resistance, can be produced at room temperatures, as opposed to the much higher melting temperatures required in the production of conventional inorganic glasses (Brinker and Scherer, 1990; Keefer, 1990). The specific uses of these sol-gel produced glasses and ceramics are derived from the various material shapes generated in the gel state, i.e., monoliths, films, fibers, and monosized powders. Many specific applications include optics, protective and porous films, optical coatings, window insulators, dielectric and electronic coatings, high temperature superconductors, reinforcement fibers, fillers, and catalysts (Keefer, 1990).

The starting materials used in the preparation of the "sol" are usually inorganic metal salts or metal organic compounds such as metal alkoxides. In a typical sol-gel process, the precursor is subjected to a series of hydrolysis and polymeration reactions to form a colloidal suspension, or a "sol". Further processing of the "sol" enables one to make ceramic materials in different forms. Thin films can

be produced on a piece of substrate by spin-coating or dip-coating. When the "sol" is cast into a mold, a wet "gel" will form. With further drying and heat-treatment, the "gel" is converted into dense ceramic or glass articles. If the liquid in a wet "gel" is removed under a supercritical condition, a highly porous and extremely low density material called "aerogel" is obtained. As the viscosity of a "sol" is adjusted into a proper viscosity range, ceramic fibers can be drawn from the "sol". Ultra-fine and uniform ceramic powders are formed by precipitation, spray pyrolysis, or emulsion techniques.

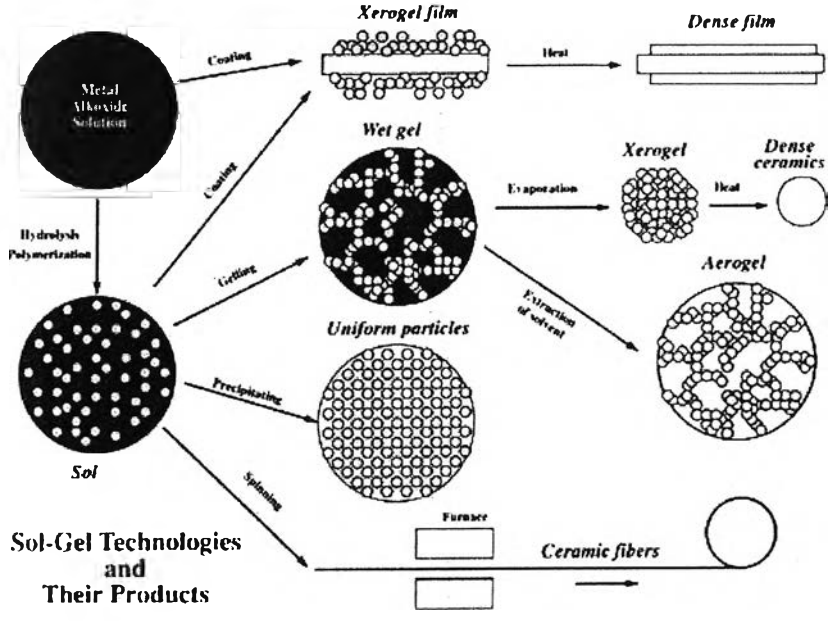

Figure 2.8 Sol-gel technology and their products

The sol-gel process, as the name implies, involves the evolution of inorganic networks through the formation of a colloidal suspension (sol) and gelation of the sol to form a network in a continuous liquid phase (gel) (Brinker and Scherer, 1990).

The precursors for synthesizing these colloids consist of a metal or metalloid element surrounded by various reactive ligands. Metal alkoxides are most popular because they react readily with water. These precursors are readily used with a suitable organic solvent, which is usually alcohol, to obtain a solution. The metal alkoxide bond is, in general, extremely susceptible to hydrolytic reaction leading to

metal hydroxides or hydrated oxides. The choice of an alkoxide can be considered by many factors including metal content, reactivity, availability, cost, decomposition temperature and sensitivity to moisture.

Intense interest has been focused on the investigation of novel metal alkoxides during the last two decades owing to their remarkable applications as precursors in the sol-gel synthesis of inorganic metal oxides for catalytic, composite and electroceramic materials, coatings and fibers. However, some significant weak points of the metal alkoxides make it difficult to investigate their structures. These drawbacks are their relatively high cost and low hydrolytic stability or high reactivity towards water. Their high reactivity is the main problem in processing inorganic oxides from alkoxides by the sol-gel method.

Many researchers have resolved these problems by modifying simple alkoxide precursors to reduce hydrolytic reactivity. However, it needs even higher cost and is not a simple way. The synthesis of new metal alkoxides possessing unique structures and properties is thus important for the study of the sol-gel process and the evolution of metal alkoxide chemistry. The precursor used in this study is prepared via the oxide one pot synthesis (OOPS) process. The precursor is inexpensive, as compared to commercially available ones, and has low hydrolytic stability. Moreover, the chemical reaction is simple and straight forward.

2.4.1 Sol gel chemistry

There are two important reactions in polymeric gel formation. These reactions are partially hydrolysis, followed by condensation polymerization. Polymerization steps via hydrolysis and condensation reactions are illustrated by the following reactions :

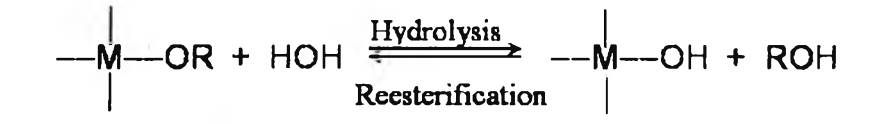

(3)

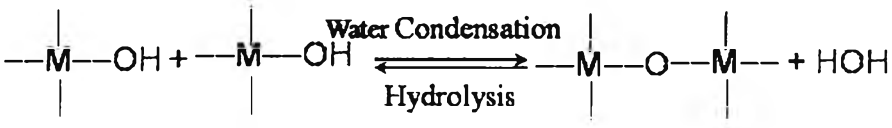

(4)

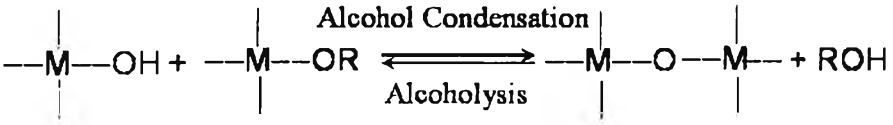

(5)

However, the characteristics and properties of a particular sol-gel inorganic network are related to a number of factors that affect the rate of hydrolysis and condensation reactions, such as, pH, temperature and time of reaction, reagent concentrations, catalyst nature and concentration, hydrolysis ratio (R), aging temperature and time, and drying (Prassas and Hench, 1984).

Of the factors listed above, pH, nature and concentration of catalyst, hydrolysis ratio (R), and temperature have been identified as most important (Keefer, 1990; Prassas and Hench, 1984). Thus, by controlling these factors, it is possible to vary the structure and properties of the sol-gel-derived inorganic network over wide ranges (Brinker, 1988).

2.5 Effect of addition of Al_2O_3 to CeO_2-ZrO_2 mixed oxides

Given the importance of the textural stability for practical application of the CeO_2-ZrO_2 in the TWCs, the design of nano composites where the CeO_2-ZrO_2 phase is dispersed over a stable inert support could represent a suitable way to improve thermal stability of these systems. Relatively few publications have been devoted to this topic and only recently the effects of addition of Al_2O_3 on the thermal stability and reduction behavior of CeO_2-ZrO_2 mixed oxides have been reported (Monte *et al.*, 2000, Yao *et al.*, 1997, Fernandez-Garcia *et al.*, 2001, and Martinez-Arias *et al.*, 2001).

It is usual practice to employ pre-formed CeO_2 or CeO_2-ZrO_2 particles to make the TWCs. These particles are then suspended with Al_2O_3 and the other components, and finally wash coated on the honeycomb. Optimized synthesis procedures are needed to produce single-phase CeO_2-ZrO_2 products at the surface of Al_2O_3 (Kaspar *et al.*, 1999). The above suggested criterion for detection of single-phase products can be conveniently employed also for Al_2O_3-supported products (Monte *et al.*, 2000).

A perusal of the data reported in the literature shows that simple impregnation of Al_2O_3 with nitrates of ceria and zirconia is ineffective in producing homogeneous products, which apparently is due to the fact that ZrO_2 tends to spread

as an amorphous layer over the surface of Al_2O_3 (Yao *et al.*, 1997). Use of a complexing agent (citric acid) (Monte *et al.*, 2000) or a micro emulsion co-precipitation (Fernández-García *et al.*, 2000) is necessary to obtain a reasonably good phase homogeneity of the mixed oxide, even though when the CeO_2-ZrO_2 content is increased from 10 to 33 wt%, some of the ZrO_2 tends to segregate on the Al_2O_3 surface (Fernández-García *et al.*, 2000). These difficulties are obviously higher at intermediate CeO_2-ZrO_2 compositions, where the opportunity for compositional inhomogeneities is statistically higher (Yao *et al.*, 1997). It should be noted that the use of the latter deposition technique generates fairly dispersed CeO_2-ZrO_2 particles at Al_2O_3 surface; average particle diameter of 2-3 nm was indeed detected both for 10 and 33 wt% loading of the mixed oxide (Fernández-García *et al.*, 2000).

The most important effect of the deposition of CeO_2-ZrO_2 on Al_2O_3 is certainly the increase of the thermal stability of the CeO_2-ZrO_2 mixed oxide compared to the unsupported one. This could be attributed either to a synergic stabilization between the Al_2O_3 and CeO_2-ZrO_2 phases or to the retarding effect of the Al_2O_3 on the sintering rate of the supported CeO_2-ZrO_2 phase. A particle size of 6 nm was in fact detected after such harsh calcination, which is far below the critical size of 15-20 nm that was suggested as a limiting value above which the mixed oxide tends to segregate (Colón *et al.*, 1999).

The stabilization of Al_2O_3 is also observed when either ZrO_2 (Horiuchi *et al.*, 1999) or CeO_2 (Paras *et al.*, 2000) are supported on Al_2O_3, CeO_2 being particularly effective under reducing conditions due to formation of $CeAlO_3$. Concerning the mutual interaction between the CeO_2- containing moiety and Al_2O_3, the addition of ZrO_2 plays a fundamental role in terms of oxygen storage. Dispersion of CeO_2 over Al_2O_3 and its reduction at high temperatures leads to formation of $CeAlO_3$ that cannot be easily re-oxidized (Shyu and Otto, 1989). When ZrO_2 is added in the form of solid solution, this deactivation pattern is strongly suppressed as shown in Figure 2.12 in contrast to CeO_2/Al_2O_3, $CeAlO_3$ could not be detected by XRD technique when ZrO_2 was incorporated into the nanocomposite mixed oxide.

While the stabilization effect of Al_2O_3 addition on the OSC properties of CeO_2-ZrO_2 mixed oxides appears well established, the effects on catalytic performances of precious metal containing catalysts are less clear.

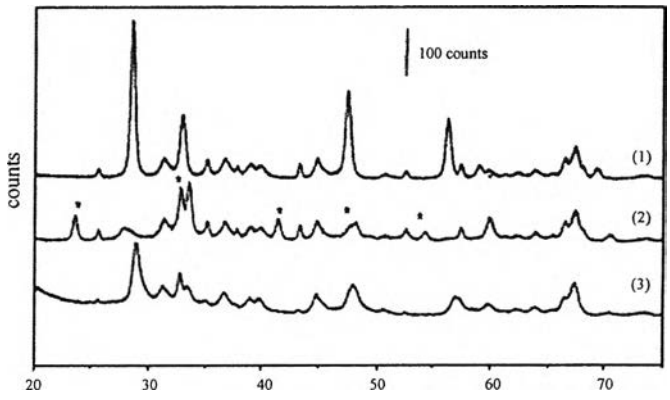

Figure 2.9 Powder XRD profiles of (1) CeO_2/Al_2O_3 calcined at 1273K for 5 h, (2) CeO_2/Al_2O_3 calcined at 1273 K for 5 h, subjected to a TPR up to 1273K followed by an oxidation at 700 K, and (3) $Ce_{0.6}Zr_{0.4}O_2/Al_2O_3$ calcined at 1273 K for 5 h, subjected to a TPR up to 1273K followed by an oxidation at 700 K. (*) peaks belonging to $CeAlO_3$

2.6 Effect of addition of copper to CeO_2-ZrO_2 mixed oxides

Carbon monoxide and gaseous hydrocarbons are ubiquitous air pollutants emitted by many sources. Complete oxidation of these pollutants to carbon monoxide and water over active catalysts is used to meet continually changing environmental regulations in an economic way. Moreover in recent years, catalytic oxidation of CO has attracted considerable attention due to many applications such as trace CO removal in the enclosed atmospheres, gas purification for CO_2 lasers, CO gas sensors, and fuel cell (Zhu *et al.*, 2004).

Noble metal catalysts such as Au, Pt, and Pd have been proved very effective for CO oxidation at low temperature (Zhu *et al.*, 2004). However, due to the high cost of noble metals and sensitivity to sulfur poisoning, more and more research is focusing on new catalysts containing cheap transition metals.

Among them, copper catalyst was found to be an excellent base metal catalyst for CO oxidation (Wang *et al.*, 2004). CuO-CeO_2 catalysts have been widely

studied for various reactions such as NO reduction, complete CO oxidation, preferential oxidation (PROX), the water-gas shift (WGS), and the wet oxidation of phenol due to high activity and selectivity for these reactions (Sedmak *et al.*, 2004).

Avgourpoulos et al. reported that $CuO\text{-}CeO_2$ catalyst had the same activity as Pt/Al_2O_3 catalyst. Sedmak et al. prepared nanostructured $Cu_{0.1}Ce_{0.9}O_{2-y}$ by a sol-gel method, which exhibited excellent activity and selectivity for preferential oxidation of CO in excess H_2 at low temperature. Due to the promising advantage of low price and high activity, $CuO\text{-}CeO_2$ catalysts are expected to substitute for the noble metal catalysts in the future.

For CO oxidation, there are two facts that govern the activity of the $CuO\text{-}CeO_2$ catalysts, namely, surface area and active sites of the catalyst. Although much attention is paid to the $CuO\text{-}CeO_2$ catalysts, $CuO\text{-}CeO_2$ catalysts with high surface area ($\geq 60\ m^2\ g^{-1}$) were rarely reported. It is well-known that a catalyst with higher surface area generally gives better catalytic activity, due to the fact that it can provide more active sites.

It was believed that CuO species are the active sites for CO oxidation however, the existing state of CuO in the $CuO\text{-}CeO_2$ catalyst is usually complex, and contribution of each CuO species to catalytic activity should be different (Luo *et al.*, 1997).

As described above, as a support ceria will result in significant efficiency decrease of the catalysts under thermally harsh environments, such as loss of surface area of the support, sintering of precious metals and deactivation of ceria. In order to improve the property of ceria, zirconia is widely used as a promoter in ceria-contained catalysts. After calcinations at high temperature (800°C), compared to pure ceria, ceria-zirconia mixed oxides shows enhanced redox and oxygen storage properties, improved thermal resistance and better catalytic activity at lower temperature.

Mart´ınez-Arias et al. investigated the redox properties and catalytic activities for CO oxidation in presence of NO of $CuO/Ce_{0.5}Zr_{0.5}O_2$ with low loading amount of copper species (1 wt%), and they proposed that the two basic factors affecting the catalytic performance of this system were the facility for achieving a

partially reduced state for the copper oxide phase at the interfacial zone and the redox properties of the $CuO_x/Ce_{0.5}Zr_{0.5}O_2$ interface.

Despite of many studies on ceria-zirconia solid solution and the CuO supported on ceria-zirconia solid solution mentioned above, the nature of interaction between the active species (copper oxide) and the support (ceria-zirconia solid solution) is still indistinct and widely open to study.